IOP Conference Series: Materials Science and Engineering

PAPER • **OPEN ACCESS**

Germanium Atom Substitution in Monolayer Graphene:A First-principles Study

To cite this article: Muhammad Rafique *et al* 2018 *IOP Conf. Ser.: Mater. Sci. Eng.* **422** 012010

Germanium Atom Substitution in Monolayer Graphene:A First-principles Study

Muhammad Rafique[(a),b)*)], Shuai Yong[(b)], Irfan Ali[(c)] and Irfan Ahmed[(a)]

[(a),*)]Mehran University of Engineering and Technology, S.Z.A.B, Campus Khairpur Mir's, Sindh, Pakistan
[(b)]School of Energy Science and Engineering, Harbin Institute of Technology,92 West Dazhi Street, Harbin 150001, PR China
[(c)]Institute of Chemistry, Shah Abdul Latif University, Khairpur Mirs', Pakistan

E-mail:shuaiyong@hit.edu.cn

Abstract. In this work, structure, electronic and optical parameters of germanium (Ge) atom substituted monatomic graphene are demonstrated through first-principles study (FPS) computations. The concentration of Ge atoms was changed from 2.5 % to 7.5 % and the effects of varying concentration on aforementioned properties were investigated. It is observed that, replacing C atoms with Ge in graphene leads to a finite bandgap opening at the Dirac K-point, thereby producing a direct bandgap semiconducting graphene. We also found that, Ge doping in graphene significantly changes its refractive index parameter. Moreover, Ge atom doping in graphene reduces the overall absorption coefficient, though it observes a considerable red-shift towards the visible region of spectrum. Graphene reflectivity improves in low lying energy region after Ge atom substitution in its lattice. These results can pave a new route for tuning the electronic and optical properties of graphene to make it functional for nanoelectronics and optoelectronic device applications.

1. Introduction

Ever since the first report on graphene in 2004 [1], a sufficient amount of work and time has been attributed by the researchers to manipulate the intrinsic properties of this fascinating material to make it useful for real engineering applications. The electronic structure of graphene can be modified by chemically doping or adsorbing foreign atoms onto graphene. These foreign atoms can work as accepter or donor impurities in the graphene structure which can move the Fermi energy level (E_F) up or down depending upon the nature of impurity atoms/clusters [2,3]. Some studies [4,5] reveal that semiconducting graphene can be obtained, when nitrogen (N) or boron (B) atoms are incorporated in its lattice. Since graphene contains zero bandgap but Ge atom is a wide bandgap semiconductor; Hence substitution of Ge atom in graphene is a natural proposition for producing an ample and well-defined bandgap in monolayer graphene [6,7].

It is well known that, pure graphene absorbs 2% of light in the visible region [8]. Functionalizing graphene for absorbing specific wavelength of spectra, it is crucial to alter the absorption spectrum of graphene to make it practical for optoelectronic devices. Sedelnikova et al. [9] and Marinopoulos et al. [10] have comprehensively examined the optical properties for rippled graphene and flat boron nitride (BN) sheet, respectively. Some FPS calculations have been performed on the electronic and optical characteristics of intrinsic and extrinsic graphene and graphynes [11-16]. These studies reveal that, doping hetro atoms in graphene and graphynes can transform the intrinsic parameters of host materials.

Very recently, M. L. Ould Ne et al. [11] performed some FPS calculations on Ge atom-doped graphene structures. Authors reveal that, by introducing Ge atom in graphene lattice a well-defined bandgap in graphene electronic structure can be achieved. Though, in this study the concentration of host C atoms is varied while dopant impurity is kept constant. Hence, in this paper we try to explore the effects of variation in the concentration of impurity atoms on the intrinsic properties of graphene while keeping the supercell size as constant.

2. Details of computation

DFT calculations are performed on Ge atom-doped graphene structures, through GGA approach implemented in Vienna Ab-initio simulation package (VASP) [17,18]. VASP utilizes PAW potentials [19] with PBE functional [20] of exchange-correlation. A 450 eV kinetic energy cut-off was utilized for the expansion of wave function. A Graphene 5 × 4 supercell structure was used in this work with varying concentration of Ge atoms present in its lattice. 15 Å vacuum layer thickness in the Z direction is applied in order to eradicate the interaction between nearby layers. For Brillouin zone (BZ) sampling, we adopted Γ-centered 9 × 9 × 1 k-point grid. Given structural models were relaxed completely until less than 0.01 eV/Å Hellmann–Feynman forces and the energy change less than 10^{-6} eV was gained, respectively. To satisfy partial occupancy problems we utilized Gaussian smearing method.

3. Results and discussions

3.1. Formation energies of Ge doped graphene

Reliability of all Ge atom-doped graphene systems can be verified by calculating the formation energy; which can be obtained through following expression [21],

$$\mathbf{E_{(gpGe)}} = \mathbf{E_{(gpGe)}} - \mathbf{E_{pgp}} + \mathbf{m}\mu_{\mathbf{c}} - \mu_{\mathbf{Ge}} \quad (\mathbf{1})$$

here, terms $\mathbf{E_{pgp}}$ and $\mathbf{E_{(gpGe)}}$ are the total energies of pure and Ge atom-doped graphene structures, respectively. The chemical potentials of carbon $\mu_{\mathbf{c}}$ and germanium $\mu_{\mathbf{Ge}}$ were gained through pristine graphene and standard phase of Ge crystal structure [22]. The **m** represents number of C atoms replaced by **n** number of Ge atoms in its lattice. The formation energy values of -0.96 eV, -2.83 eV and -3.96 eV were obtained for 1 Ge, 2 Ge and 3 Ge substituted graphene complexes, respectively. The negative formation energies suggest that, Ge atom substitution in graphene lattice is thermodynamically favorable. The trends of the obtained formation energies of Ge doped graphene systems are consistent with earlier available reports [23].

3.2. Structural and electronic parameters of Ge substituted graphene

In this work, we investigated the effects of Ge atom substitution on aforementioned parameters. Ge atoms with varying concentration of 2.5% (1 Ge atom), 5% (2 Ge atoms) and 7.5% (3 Ge atoms) were incorporated in graphene lattice containing 40 host C atoms, respectively. Optimized geometry of 1 Ge, 2 Ge and 3 Ge atom-doped monolayer graphene is presented in Figs. 1(a)-(c), respectively. Due to larger difference between covalent radius of Ge (120 pm) and C atom (73 pm), the increase in the lattice constant of graphene occurs. Larger covalent radius of Ge atom causes local deformation in the graphene lattice, which in turn produces variation in the C-C atom bond length. In order to investigate the variations in C-C atoms bond length after Ge atom substitution, the C atoms present around the Ge impurities were not fixed, rather, were allowed to settle down during geometry relaxation.

Given Fig. 1 presents the bond distances for Ge-C and C-C constituent atoms, it is found that, during geometry relaxation process the 2D planar structure of the graphene was retained after Ge atom substitution in its lattice. Ge atoms form strong covalent bonds with adjacent C atoms via sp^2 hybridization process. Constituent C-C atom bond distances present in vicinity of Ge atoms were calculated in variety of 1.27-1.36 Å and obtained disparity in C-C atoms bond length was in variety of 0.14 Å to 0.06 Å. Bond distances of Ge-C atoms were obtained in range of 1.61-1.67 Å. In addition, Ge atom substitution produced Jahn-Teller distortion in graphene lattice by lowering the D_{3h} local

symmetry of graphene to C_{3v}, C_s or C_i symmetry during relaxation process. This calculation is in consensus with statement that, three equatorial bond distances of Ge-C atoms are different [16, 24].

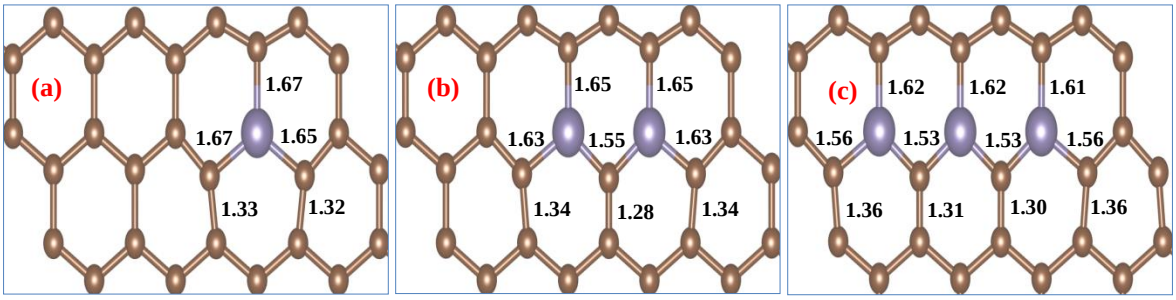

Figure 1. Top views of atomic structures Ge doped graphene systems showing bond length of Ge–C and C–C atoms in Å.

Next, the electronic structure of individual varying concentration of Ge atom-doped graphene systems is investigated. Band structure diagrams were obtained for all Ge doped graphene complexes. 30 *k*-point were adopted for each symmetrical line through path *Γ*- *M* - *K* - *Γ* in irreducible BZ for electronic structure calculation with refined grid.

Different Ge (1 Ge, 2 Ge and 3 Ge) atom-doped graphene system band structure diagrams are described in Figs. 2(a)-(c), respectively.

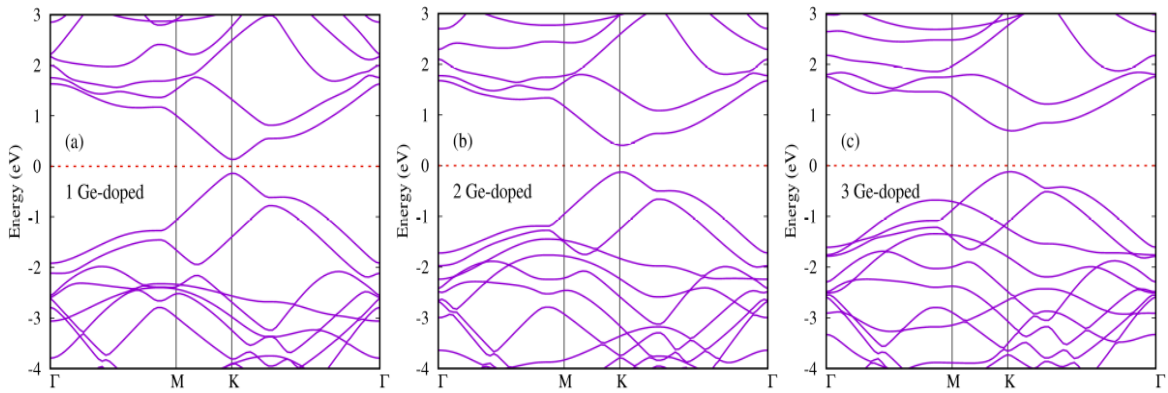

Figure 2. Electronic structure of Ge atom-doped graphene (5 × 4) supercell systems.

As we know that, Ge impurity atoms carry extra charge carriers than host C atom, so the valence electrons of Ge atoms hybridize with π* electrons of graphene. Since Ge atoms form covalent bonding with C atoms of graphene, which causes the disruption in the symmetric structure of graphene, thereby inducing a finite band gap in its electronic structure [7, 25]. Moreover, the bandgap value induced in the electronic structure of graphene is in direct proportion to number of Ge atoms present in its lattice, which is also evident in the electronic structures shown in Figs. 2(a)-(c), respectively. Single Ge atom substitution in graphene introduced a bandgap of ~0.22 eV at the Dirac point, that is consistent with earlier reports [25, 26]. When the concentration of Ge atoms present is graphene lattice is increased to 5% (i.e. 2 Ge atoms) and7.5% (i.e. 3 Ge atoms), the bandgap value increases to ~0.8 eV and ~1.1 eV, respectively. Obtained results suggest that an ample and well-defined bandgap in graphene electronic structure can be achieved by doping Ge atoms in its lattice. During Ge atom substitution in graphene, the π band of graphene stands firm at approximately -0.03 eV energy, although π* band creeps into conduction band and away from the (E_F) level depending upon the number of Ge atoms present in graphene lattice. This behaviour suggests that, the Ge atom p orbital electrons add their energy into conduction band, thereby altering the position of conduction band minimum (CBM). By increasing the concentration of dopant atoms, some extra energy is added to CBM, which in turn modifies the position of CBM in the electronic structure, thus increasing the

existing energy difference between the valence band and conduction band [11]. These predictions are consistent with the previous reports [26-28].

3.3. Optical parameters of Ge substituted graphene

Finally, we investigated the optical parameters of Ge atom-doped graphene systems through Random Phase Approximation (RPA) [29] technique within DFT scheme. Local field effects are omitted and interband transitions are included in this method. Hence, some inaccuracies in dielectric constant can be expected at low energies. To calculate the refractive index, absorption coefficient and reflectivity plots, we require dielectric constant. Since, dielectric constant is summation of real and imaginary parts i.e. $\varepsilon = \varepsilon' + \mathbf{i}\varepsilon''$ together. From dielectric constant, we can simply extract the refractive coefficient 'n', extinction coefficient 'k', absorption coefficient 'α' and reflectivity 'R'. Calculation technique for these optical properties is demonstrated in detail in Ref. [10]. Our obtained optical parameters for pure graphene are consistent with previous reports [8, 9, 30].

Figs. 3(a) and 3(b) present the refractive index plots for pure and Ge atoms substituted graphene structures and the comparison is also provided. Static refractive index (i.e. value of refractive index at zero energy) for pure graphene is found as 2.75, and its smallest peak appears at 5 eV energy. Though, after Ge atom substitution, static refractive index value is increased. During single Ge atom substitution, static refraction index (n) value increases to ~3.6 as given in Fig. 3(a).

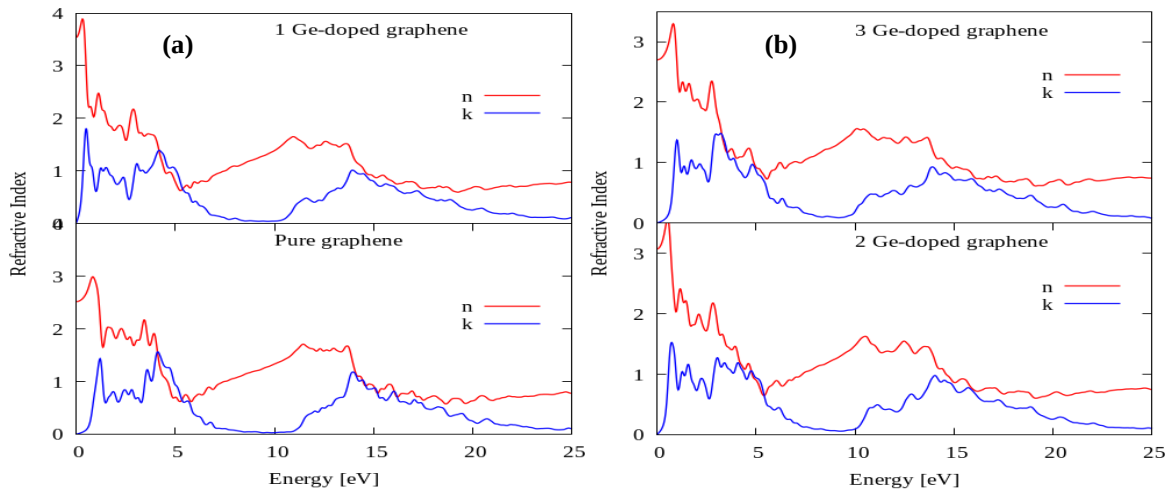

Figure 3. Refractive Index of (a) Pure, 1 Ge atom-doped and (b) 2 and 3 Ge-atom doped graphene

Likewise, pure graphene extinction coefficient (k) maximum peaks emerge at 1 eV and 5 eV energy with 1.4 and 1.6 peak intensities. However, after single Ge atom-doping, the first maximum peak shifts to lower energy at 0.7 eV with 1.85 peak intensity. This behaviour suggests that Ge atom substitution can produce shift in the extinction coefficient towards lower energy and also produces increment in the peak intensity of extinction coefficient as shown in Fig. 3(a), respectively. When concentration of Ge atoms is increased to 5% and 7.5%, similar changes in static 'n' and 'k' values as mentioned above are achieved as described clearly in Fig. 3(b). To sum up, one can assume that Ge atom incorporation in graphene can significantly change the refractive coefficient (n) and extinction coefficient (k) parameters of graphene.

Pure and Ge atom substituted graphene system absorption coefficient plots are presented in Fig. 4(a), respectively. Two major absorption peaks emerging at ~4.5 eV, ~14 eV energy levels having intensity of ~3500 cm^{-1} and 8700 cm^{-1} are observed in pure graphene absorption spectrum as evident in 4(a), respectively [31]. The first peak at 4.5 eV is associated with $\pi \rightarrow \pi^*$ transitions and the second peak appearing at 14 eV is associated with $\sigma \rightarrow \sigma^*$ transitions. Moreover, zero absorption coefficient quantity is obtained in the energy range of 0-0.5 eV and also from 7-11 eV for pure graphene system [8, 32]. However, when Ge is embedded in graphene, it enables absorption coefficient parameter to start from ~0 eV energy, indicating, Ge doping can produce red shift in the absorption spectrum of pure graphene which is evident in 4(a). Similarly, some changes in the absorption quantity values are

also achieved in 7-11 eV energy intervals. During Ge atom incorporation in graphene, highest absorption peak attributed to σ→σ* transitions appearing at 14 eV for pure graphene attains lesser values and the smallest absorption peak attributed to π→π* appearing at ~4.5 eV is drifts towards low energy range. Through obtained absorption coefficient parameter, one can predict that Ge atom incorporation in graphene, reduces the absorption quantity as a whole; Though, provides a red-shift in absorption spectrum towards visible region.

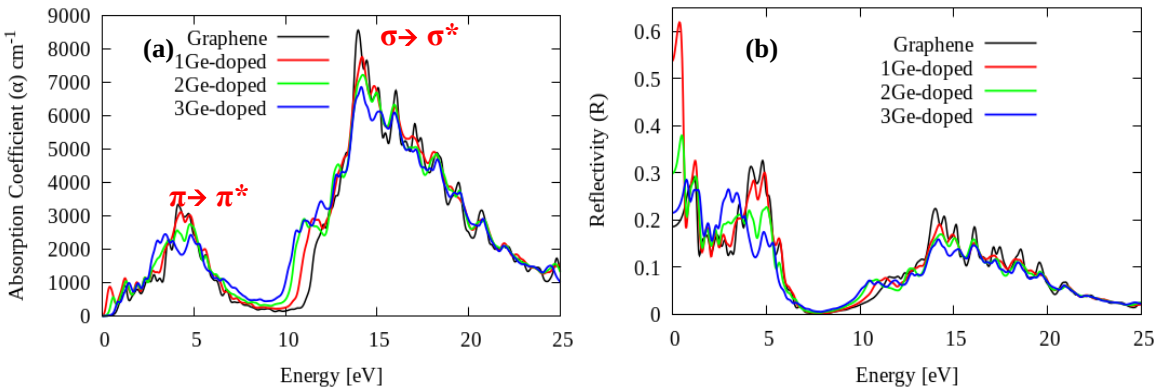

Figure 4. (a) Absorption coefficient and (b) Reflectivity plot of pure and Ge substituted graphene systems

Fig. 4(b) describes the reflectivity diagram for pure and Ge substituted graphene systems. The reflectivity plot of intrinsic graphene contains three main peaks with ~0.29, 0.32 and 0.21 intensities at ~0.7 eV, ~4.5 eV and ~14 eV energy levels as presented in Fig. 4(b), respectively [8, 32]. However, when Ge atoms are incorporated into graphene, the two main peaks emerging at ~4.5 eV and ~14 eV present reduced intensity values as the concentration of Ge atom is increased which is evident in Fig. 4(b). Additionally, the low lying energy reflectivity peak of pure graphene appearing at 0.7 eV with 0.29, intensity has increased intensity of approximately 0.62 and 0.38 for 1 and 2 Ge atom-doped monolayer graphene systems as given in Fig. 4(b), respectively. When Ge atom concentration reaches to 7.5 %, the overall reflectivity parameter shows diminishing behaviour. It can be concluded that, introduction of Ge atoms in graphene lattice, provides increase in the static reflectivity (R at 0 eV) while the reduction in reflectivity in higher energy region is achieved as presented in Fig. 4(b), respectively [8, 32].

4. Conclusions

The structural, electronic and optical parameters for Ge doped graphene structures were investigated using FPS calculation based on DFT method. The concentration of Ge atoms was varied from 2.5 % to 7.5 % and their effects were analyzed. It is revealed that, Ge atom incorporation in graphene makes it display direct bandgap semiconductor with bandgap value of ~0.22 eV, ~0.8 eV and ~1.1 eV for 1 Ge, 2 Ge and 3 Ge atom doped graphene systems, respectively. For optical parameter calculations, it is found that, n and k peak intensities have increased values after Ge atoms substitution in graphene lattice. It is also found that, the minimum absorption peak associated to π→π* transitions appearing at 4.5 eV energy in graphene absorption spectrum exhibits a red shift in between ~0.1-0.3 eV energy towards visible range of spectrum when Ge atoms are placed in its lattice. Also the absorption coefficient appears at 0 eV energy after Ge atom doping. Similarly, reduced reflectivity parameter in higher energy region is gained while higher peak intensities in the lower energy region are obtained after Ge atom substitution into graphene. In summary, we can suggest that, Ge incorporation in graphene can produce direct bandgap semiconducting graphene. Moreover, Ge atom doping in graphene produces new trends in its optical absorption. These results pave a new route for graphene to be functional in the fields of photonics and nanoelectronics.

5. Acknowledgments

This work was supported by the Higher Education Commission, Pakistan under SRGP (No:21-1778/SRGP/R&D/HEC/2017). In addition, we would like to acknowledge the support that NVIDIA provided us through the GPU Grant Program.

6. References

[1] K. S. Novoselov, A. K. Geim, S. V. Morozov, D. Jiang, Y. Zhang, S. V. Dubonos, I. V. Grigorieva and A. A. Firsov, science **306** (5696), 666-669 (2004).
[2] P. Rani and V. Jindal, RSC Advances **3** (3), 802-812 (2013).
[3] R. Nascimento, J. d. R. Martins, R. J. Batista and H. Chacham, The Journal of Physical Chemistry C **119** (9), 5055-5061 (2015).
[4] L. Ci, L. Song, C. Jin, D. Jariwala, D. Wu, Y. Li, A. Srivastava, Z. Wang, K. Storr and L. Balicas, Nature materials **9** (5), 430-435 (2010).
[5] T. Martins, R. Miwa, A. J. Da Silva and A. Fazzio, Physical review letters **98** (19), 196803 (2007).
[6] X. Miao, S. Tongay, M. K. Petterson, K. Berke, A. G. Rinzler, B. R. Appleton and A. F. Hebard, Nano letters **12** (6), 2745-2750 (2012).
[7] P. A. Denis, ChemPhysChem **15** (18), 3994-4000 (2014).
[8] P. Rani, G. S. Dubey and V. Jindal, Physica E: Low-dimensional Systems and Nanostructures **62**, 28-35 (2014).
[9] O. Sedelnikova, L. Bulusheva and A. Okotrub, The Journal of chemical physics **134** (24), 244707 (2011).
[10]. A. Marinopoulos, L. Reining, A. Rubio and V. Olevano, Physical Review B **69** (24), 245419 (2004).
[11] M. O. Ne, A. Abbassi, A. Benyoussef, H. Ez-Zahraouy and A. El Kenz, Optical and Quantum Electronics **49** (6), 218 (2017).
[12] S. Chopra, ChemPhysChem **16** (9), 1948-1953 (2015).
[13] S. Chopra, RSC Advances **6** (25), 20565-20570 (2016).
[14] S. Chopra and L. Maidich, RSC Advances **4** (92), 50606-50613 (2014).
[15] R. Muhammad, Y. Shuai and H.-P. Tan, Physica E: Low-dimensional Systems and Nanostructures (2016).
[16] J. Liu, Z. Xin, X. Yan, H. Li and M. Yu, Solid State Communications **258**, 38-44 (2017).
[17] G. Kresse and D. Joubert, Physical Review B **59** (3), 1758 (1999).
[18] G. Kresse and J. Furthmüller, Computational Materials Science **6** (1), 15-50 (1996).
[19] P. E. Blöchl, Physical Review B **50** (24), 17953 (1994).
[20] J. P. Perdew, K. Burke and M. Ernzerhof, Physical review letters **77** (18), 3865 (1996).
[21] D. Li, C. Wang, Y. Niu, H. Zhao and C. Liang, Chemical Physics Letters **601**, 16-20 (2014).
[22] M. Rafique, Y. Shuai, H.-P. Tan and H. Muhammad, Applied Surface Science **408**, 21-33 (2017).
[23] P. A. Denis, Computational and Theoretical Chemistry **1097**, 40-47 (2016).
[24] E. Beheshti, A. Nojeh and P. Servati, Carbon **49** (5), 1561-1567 (2011).
[25] M. S. Azadeh, A. Kokabi, M. Hosseini and M. Fardmanesh, Micro & Nano Letters **6** (8), 582-585 (2011).
[26] E. Aktürk, C. Ataca and S. Ciraci, Applied Physics Letters **96** (12), 123112 (2010).
[27] T. Cui, R. Lv, Z.-H. Huang, S. Chen, Z. Zhang, X. Gan, Y. Jia, X. Li, K. Wang and D. Wu, Journal of Materials Chemistry A **1** (18), 5736-5740 (2013).
[28] Z. Liu, J. Li, Z.-H. Sun, G. Tai, S.-P. Lau and F. Yan, ACS nano **6** (1), 810-818 (2011).
[29] M. Gajdoš, K. Hummer, G. Kresse, J. Furthmüller and F. Bechstedt, Physical Review B **73** (4), 045112 (2006).
[30] A. Laref, A. Ahmed, S. Bin-Omran and S. Luo, Carbon **81**, 179-192 (2015).
[31] M. Rafique, Y. Shuai, H.-P. Tan and M. Hassan, RSC Advances **7** (27), 16360-16370 (2017).
[32] R. Muhammad, Y. Shuai and H.-P. Tan, Physica E: Low-dimensional Systems and Nanostructures **88**, 115-124 (2017).